A small molecule inhibitor of RNA-binding protein IGF2BP3 shows anti-leukemic activity

Amit K. Jaiswal,[1] Georgia M. Scherer,[2+] Michelle L. Thaxton,[1+] Jacob P. Sorrentino,[2] Constance Yuen,[3] Milauni M. Mehta,[2] Gunjan Sharma,[1] Tasha L. Lin,[1] Tiffany M. Tran,[1] Amanda Cohen,[1] Alexander J. Ritter,[4] Rishi S. Kotecha,[5-7] Jeremy R. Sanford,[4,8] Robert D. Damoiseaux,[3,9-11] Neil K. Garg[2] and Dinesh S. Rao[1,11,12]

[1]Department of Pathology and Laboratory Medicine, University of California, Los Angeles, CA, USA; [2]Department of Chemistry and Biochemistry, University of California, Los Angeles, CA, USA; [3]California Nanosystems Institute, University of California, Los Angeles, CA, USA; [4]Department of Molecular, Cell and Developmental Biology and Center for Molecular Biology of RNA, University of California, Santa Cruz, CA, USA; [5]Department of Clinical Haematology, Oncology, Blood and Marrow Transplantation, Perth Childrens Hospital, Perth, Western Australia, Australia; [6]Leukemia Translational Research Laboratory, WA Kids Cancer Centre, University of Western Australia, Perth, Western Australia, Australia; [7]Curtin Medical School, Curtin University, Perth, Western Australia, Australia; [8]Center for Biomolecular Science & Engineering, University of California, Santa Cruz, CA, USA; [9]Department of Molecular and Medical Pharmacology, University of California, Los Angeles, CA, USA; [10]Department of Bioengineering, Samueli School of Engineering, University of California, Los Angeles, CA, USA; [11]Jonsson Comprehensive Cancer Center, University of California, Los Angeles, CA, USA and [12]Broad Stem Cell Research Center, University of California, Los Angeles, CA, USA

[+]*GMS and MLT contributed equally.*

Correspondence: D.S. Rao
drao@mednet.ucla.edu

Received: May 14, 2025.
Accepted: November 18, 2025.
Early view: November 27, 2025.

https://doi.org/10.3324/haematol.2025.288221

Abstract

The RNA-binding protein IGF2BP3 is an oncofetal protein over-expressed in B-cell acute lymphoblastic leukemia and is critical for leukemogenesis in experimental models. With cancer-specific expression, functional dispensability for normal development, and an unleveraged pro-oncogenic function in mRNA homeostasis, IGF2BP3 represents an excellent target. With no small molecule inhibitors of IGF2BP3 in clinical use, we aimed to identify new IGF2BP3 inhibitors using biochemical methods. A biochemical screen, followed by a cell-based counter screen led to the identification of compounds with protein-RNA interaction inhibition and leukemic cell growth-inhibitory activity. One of these compounds, designated I3IN-002, shows consistent cell growth-inhibitory activity, altered cell cycle, and increased apoptosis in multiple leukemia cell lines, and is the most potent inhibitor of IGF2BP3 reported to date. I3IN-002 was tolerated in mice when administered intraperitoneally and showed potent anti-leukemic activity in a syngeneic transplantation model of MLL-Af4 leukemia. I3IN-002 inhibits the function of IGF2BP3, disrupting *in situ* binding of IGF2BP3 to target mRNA, and altering IGF2BP3-dependent gene expression regulation. Furthermore, cell-free and cellular thermal shift assays, as well as drug affinity responsive target stability assays support on-target activity of I3IN-002 for IGF2BP3. Thus, the identification of I3IN-002 paves the way for the discovery of potent and selective small molecule inhibitors of IGF2BP3.

Introduction

RNA binding proteins (RBP) are important players in post-transcriptional gene regulation, and many show cancer-specific expression and may regulate oncogenesis via diverse mechanisms.[1-5] The RNA binding protein IGF2BP3 was initially discovered as a factor over-expressed in pancreatic cancer and one of three homologous proteins (IGF2BP1-3) that bound to the 5'-untranslated region of the IGF2 mRNA.[1] Since its original description, a large body of work has congruently demonstrated its role as an oncogenic protein in a number of different cancers, and that IGF2BP3 binds to the 3'UTR of mRNA.[2,3] In acute leukemia, we and others initially identified IGF2BP3 as an up-regulated RBP

in MLL-translocated B-ALL.[4,5] IGF2BP3 is transcriptionally induced by MLL-AF4, and overexpression of IGF2BP3 in bone marrow led to hyperproliferation in hematopoietic stem and progenitor cells (HSPC) in mice.[4] Moreover, deletion of *Igf2bp3 in vivo* significantly limited leukemia development and increased leukemia-free survival.[4,6,7] At baseline, the *Igf2bp3* knockout mouse did not show any overt phenotypes, suggesting that it is not essential for normal development and homeostasis in the adult. Taken together, these studies established IGF2BP3 as an oncogenic target in acute leukemia.

To investigate the molecular mechanisms of IGF2BP3's action, we had previously undertaken eCLIP-seq, a technique designed to globally detect RNA molecules bound by IGF2BP3 in conjunction with differential expression analyses in cells that were depleted for IGF2BP3. These analyses revealed that IGF2BP3 most commonly binds to the 3'UTR of mRNA transcripts. The regulated mRNA transcripts included numerous down-regulated oncogenes such as *HOXA9*, *CDK6*, and *MYC*.[4,6] Determinants of IGF2BP3-RNA binding include not only primary sequence but also epitranscriptomic modification of target mRNA with N6-methyladenosine (m^6A) and spacing between short recognition sequences.[6,8-11] Importantly, deletion of the RNA-binding domains of IGF2BP3 abrogated stabilization of these transcripts, and reversed IGF2BP3-driven pre-leukemic disease *in vivo*.[4] Together these data suggest that IGF2BP3's binding to specific mRNA is central to its role in promoting oncogenesis in the hematopoietic system. RNA binding proteins were previously under-represented in targeted therapy approaches due to their presumed "undruggable" status; however, recent efforts have uncovered small molecules targeting RBP, including the IGF2BP family.[4,12] With the oncogenic role of IGF2BP3 established by not only our studies but also from numerous other studies in literature, we sought to identify a small molecule inhibitor of the protein. To this end, we developed and validated a time-resolved Förster resonance energy transfer (TR-FRET) assay, using purified IGF2BP3 protein and a synthetic m^6A-modified target RNA molecule to measure binding. A library of small molecule compounds was applied to this assay, with resultant hit compounds being re-confirmed in TR-FRET assays and counter screened in cell-based assays. Confirmatory studies demonstrate activity in several leukemia cell lines with IGF2BP3 overexpression showing inhibition of cell growth and cell cycle progression, and increased apoptosis. One of these hit compounds, referred to here as I3IN-002, shows activity against leukemic initiating cells *in vitro*, and has anti-leukemic activity *in vivo*. I3IN-002 directly interferes with the function of IGF2BP3, as assessed by gene expression analyses and RNA immunoprecipitation experiments that measure IGF2BP3-dependent gene expression and IGF2BP3-mRNA binding. Furthermore, cellular thermal shift assays, cell-free thermal shift assay (TSA), and drug affinity responsive target stability (DARTS) support on-target activity for I3IN-002. I3IN-002 may prove useful as a tool compound in future biochemical studies involving IGF2BP3, and may also enable the development of novel therapeutics for the treatment of leukemia and other hematologic cancers.

Methods

Cell lines and cell culture

All cell lines were maintained in standard conditions in an incubator at 37°C and 5% CO_2. Human B-ALL cell lines, RS4;11 (ATCC CRL-1873), NALM6 (ATCC CRL-3273), SEM (DMZ-ACC 546), PER785, REH (ATCC CRL-8286), OCI-AML 8227 and KASUMI-2 (DSMZ ACC 526), and immortalized MLL-Af4 transformed murine HSPC were cultured as previously described.[6] A full list of reagents is provided in *Online Supplementary Table S1*.

Antibodies

Antibodies were used for western blotting, FACS, and immunoprecipitation experiments as described.[4,13,14] A list of antibodies is provided in *Online Supplementary Table S2*.

Protein purification and high throughput assays

IGF2BP3-GFP-Flag overexpression plasmid was constructed by fusing full length IGF2BP3 coding sequence (CDS) with GFP CDS and Flag CDS, and cloning in pCDNA 3.0 vector. Protein was purified using standard methods and anti-Flag based affinity purification. Purified protein was added to pre-incubated Streptavidin-terbium plus biotinylated m^6A-labeled RNA oligonucleotide (*Online Supplementary Table S3*). The plate was incubated for 1 hour at room temperature for binding and read on an EnVision microplate reader (Perkin Elmer) with a dual PMT configuration using a 340 nm excitation and a dual emission mirror block with a 495 nm emission filter for Terbium fluorescence (W1 channel) and a 525 nm emission filter for GFP fluorescence (W2 channel). The assay was miniaturized to 10 uL in 384-well plates and an in-house compound deck library at the UCLA MSSR was applied to the assay. Data analysis was performed as described in the *Online Supplementary Methods*.

Counter-screen and cell-based assays

Wild-type (WT) and IGF2BP3-deleted SEM cell lines[6] were treated with compound, grown for four days under normal growth conditions, and assayed for cell growth in 384-well plates with CellTiter-Glo, a luminescence-based reagent described previously.[6,13,14] Following identification of lead compounds, further measurements of apoptosis, cell cycle, and proliferation were performed as we have previously described.[6,13,14]

Compound synthesis

Briefly, organic synthesis was performed utilizing commer-

cially available fragments and a custom in-house strategy allowing for the design of the original compound and future analogs. A full description is provided in the *Online Supplementary Methods*.

Assays to define on-target activity

A cellular thermal shift assay was performed on SEM cells treated with the test compound, based on published protocols with minor modifications, as described in the *Online Supplementary Methods*. The thermal shift assay with purified protein, and Drug Affinity responsive target stability assays were performed as previously described.[15,16] Lastly, RNA-sequencing to define differential gene expression, as well as RNA immunoprecipitation followed by sequencing (RIP-seq), were performed using standard methods.[4,17] RNA sequencing data has been deposited in the NCBI Short read archive with accession numbers PRJNA1333638 and PRJNA1336320.

Animal experiments

For *in vivo* studies, C57BL/6J, B6.SJL-*Ptprc*^{a} *Pepc*^{b},/BoyJ (B6 CD45.1), and B6J.129(Cg)-Gt(ROSA)26Sor$^{tm1.1(CAG-cas9*,-EGFP)Fezh/J}$ (Cas9-GFP, BL/6J) mice were procured from The Jackson Laboratory. Preliminary toxicity studies were carried out to identify issues with small molecule delivery in non-transplanted mice. Primary murine leukemia cells (WT and Igf2bp3 knockout [KO]), prepared as previously described,[14] were transplanted into busulfan-conditioned recipients. I3IN-002 was delivered intraperitoneally, three times a week for three weeks. Once the peripheral blood engraftment reached >20% at four weeks, the experiment was terminated and tissues were harvested to be analyzed by FACS, histology and reverse transcription-quantitative polymerase chain reaction (RT-qPCR). A separate experiment examined overall and leukemia-free survival. All of the animal experiments received Institutional Animal Research Committee approval at the University of California, Los Angeles.

A complete description of methods can be found in the *Online Supplementary Appendix*.

Results

Disruptors of protein-RNA interactions are identified via biochemical screening

To identify putative inhibitors of IGF2BP3 (I3), we designed and validated a time-resolved Förster resonance energy transfer (TR-FRET) assay, based on binding of a GFP-tagged I3 (I3-GFP) to a biotinylated RNA oligonucleotide carrying an m^{6}A modification (Figure 1A). Small molecules that interfere with this interaction will lead to a loss of signal transfer, and subsequently decreased GFP fluorescence. For this assay, we generated a carboxy-terminal GFP- and FLAG-tagged IGF2BP3 protein-encoding mammalian expression vector (I3-GFP-F), cloned into pcDNA3.1 (*Online Supplementary Figure S1A*). We confirmed a functional fusion protein based on bright fluorescence following transfection and recognition with anti-IGF2BP3 antibodies (*Online Supplementary Figure S1B*). The protein was purified by elution from fractions 3-11 on an anti-FLAG column (*Online Supplementary Figure S1C*) and subsequently concentrated and quantitated by Coomassie staining (*Online Supplementary Figure S1D*). Functionality of the protein was confirmed by RNA immunoprecipitation of target mRNA following incubation of purified protein with cell extracts and pull-down with anti-FLAG (*Online Supplementary Figure S1E-G*). Following purification and confirmation of RNA-binding activity, we confirmed that GFP fluorescence in the TR-FRET assay required the presence of all components (i.e., I3-GFP, biotinylated mRNA, and Terbium) (Figure 1B). The assay demonstrated saturation of the GFP fluorescence signal at approximately 50 nM of I3-GFP-F and 25 nM RNA oligonucleotide (Figure 1C and *Online Supplementary Figure S1H*). Next, we evaluated assay reproducibility across multiple experiments performed across multiple days, finding excellent concordance in GFP fluorescence and Z' values (*Online Supplementary Figure S1 I, J*).

To adapt the assay to high throughput screening, we first successfully miniaturized the assay to 10 μL, while maintaining σ+ <20% and Z' >0.5, with highly reproducible GFP fluorescence (*Online Supplementary Figure S1K*). Following this validation, a high throughput screen of 196,567 compounds was completed in two stages, a preliminary screen, and a full-scale screen. We were able to successfully complete the screen: across 617 plates that were analyzed for this assay, a representative plate map is shown with and without hits (*Online Supplementary Figure S2A*). From the analysis, we achieved >99% of plates that showed standard deviation <20% and 95% of plates showed a Z' score >0.5 (Figure 1D and *Online Supplementary Figure S2B*). Plates that showed a low Z' score were excluded from downstream hit confirmation. To define hits, we leveraged the preliminary screen to increase the specificity of hit definition (*Online Supplementary Figure S2C*). Using only the primary criterion, defined as |Ratio Z|>3 (where Ratio is the ratio of terbium fluorescence/GFP fluorescence), we obtained a hit rate of 1.33% in the preliminary screen, and 1.73% in the full-scale screen (Figure 1E). Using a secondary criterion, where Terbium fluorescence ("W1") was within one standard deviation of the mean for the plate (i.e., |W1 Z|<1), the hit rate was reduced to 0.94% and 0.19% in preliminary and full-scale screens, respectively (Figure 1E). The reduced hit rate in the full-scale screen, therefore, is most likely due to increased variability in terbium fluorescence. Further refinements of hits, by an alternate secondary criterion definition (mean and standard deviation calculated for the experimental run, rather than the plate) and manual curation of the data when irregularities were observed, led to an initial, high-stringency list of 417 compounds that were further analyzed. Of the 417 hits out of 186,978 evaluable compounds, 29

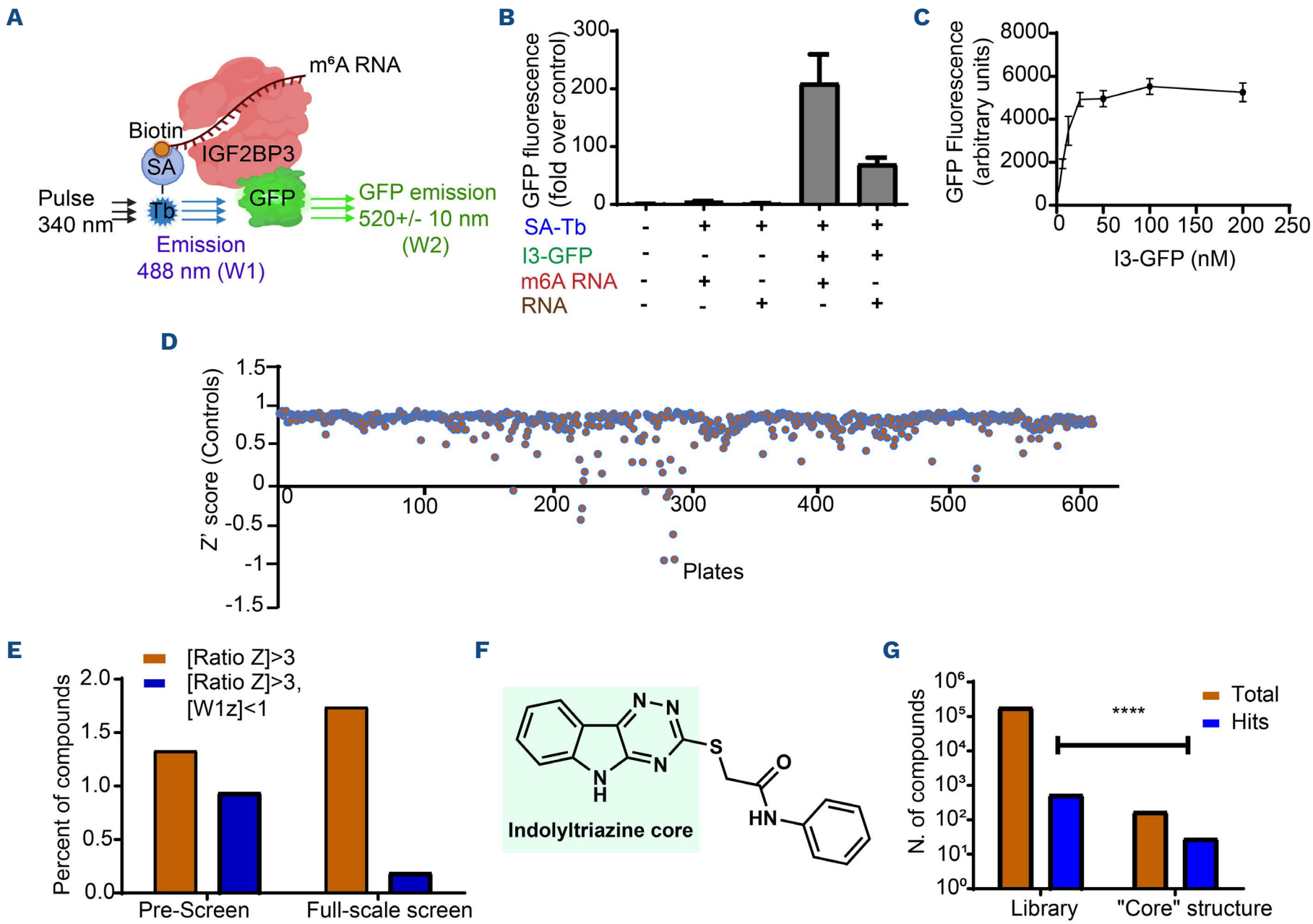

Figure 1. Design and execution of a high throughput assay to identify small molecule inhibitors of IGF2BP3. (A) Schematic of assay. IGF2BP3-GFP fusion protein is bound to an m6A-modified, biotinylated RNA oligonucleotide, which in turn is bound to Streptavidin-terbium (SA-Tb). Förster resonance energy transfer occurs when the protein and RNA are bound. (B) GFP Fluorescence (fold-change over control) plotted for different combinations of SA Tb,, IGF2BP3-GFP (I3-GFP), m^6A-modified RNA (m^6A RNA), or unmethylated, biotinylated RNA (RNA). (C) GFP Fluorescence (arbitrary units) as a function of IGF2BP3-GFP protein concentration. (D) High throughput screening assay Z' scores for control reactions across 600+ plates screening over 186,978 compounds. (E) Screening was conducted first with a limited set of compounds (preliminary screen) prior to a full-scale screen. Fluorescence ratios were calculated as W1/W2 where W1 is the Terbium fluorescence and W2 is the GFP fluorescence. Shown are the percentages of compounds satisfying a single criterion (i.e., Ratio Z) or two criteria (Ratio Z and W1 Z). (F) First "core structure" identified from the screen. The indolyltriazine substructure was conserved across multiple hits from screening in (D) and (E). (G) Comparison of total number of hits in the library *versus* hits amongst compounds containing the first core structure; Fisher's exact test, ****P<0.0001. N: number.

contained a core structure with an indolyltriazine group (Figure 1F). Remarkably, the library only contained 174 total compounds with the general structure depicted in Figure 1F, representing an approximate 74-fold enrichment for these compounds, a highly statistically significant result (P<0.0001; Fisher's exact test) (Figure 1G). Together, our results identify a number of small molecules with *in vitro* activity against the RNA binding activity of IGF2BP3.

Cell-based counter screen identifies molecules with anti-leukemic activity

To further characterize the hits identified from the screen, we first performed a confirmatory TR-FRET assay, with two experiments consisting of three replicates each. Concordant TR-FRET findings were characterized as Tier 1, 2 and 3, when findings were reproduced in 2/2, 1/2, or 0/2 experiments, respectively. In all, 89.3% (371/417) of hit compounds and 93.1% (27/29) of indolyltriazine compounds were Tier 1 or Tier 2 hits, respectively (*Online Supplementary Figure S2D*). To further examine these confirmed hits, we turned to a cell-based assay (Figure 2A). Here, we reasoned that a compound that was specific for IGF2BP3 would only show activity in SEM cell lines that contained intact, increased expression of the protein (SEM-WT), with reduced activity

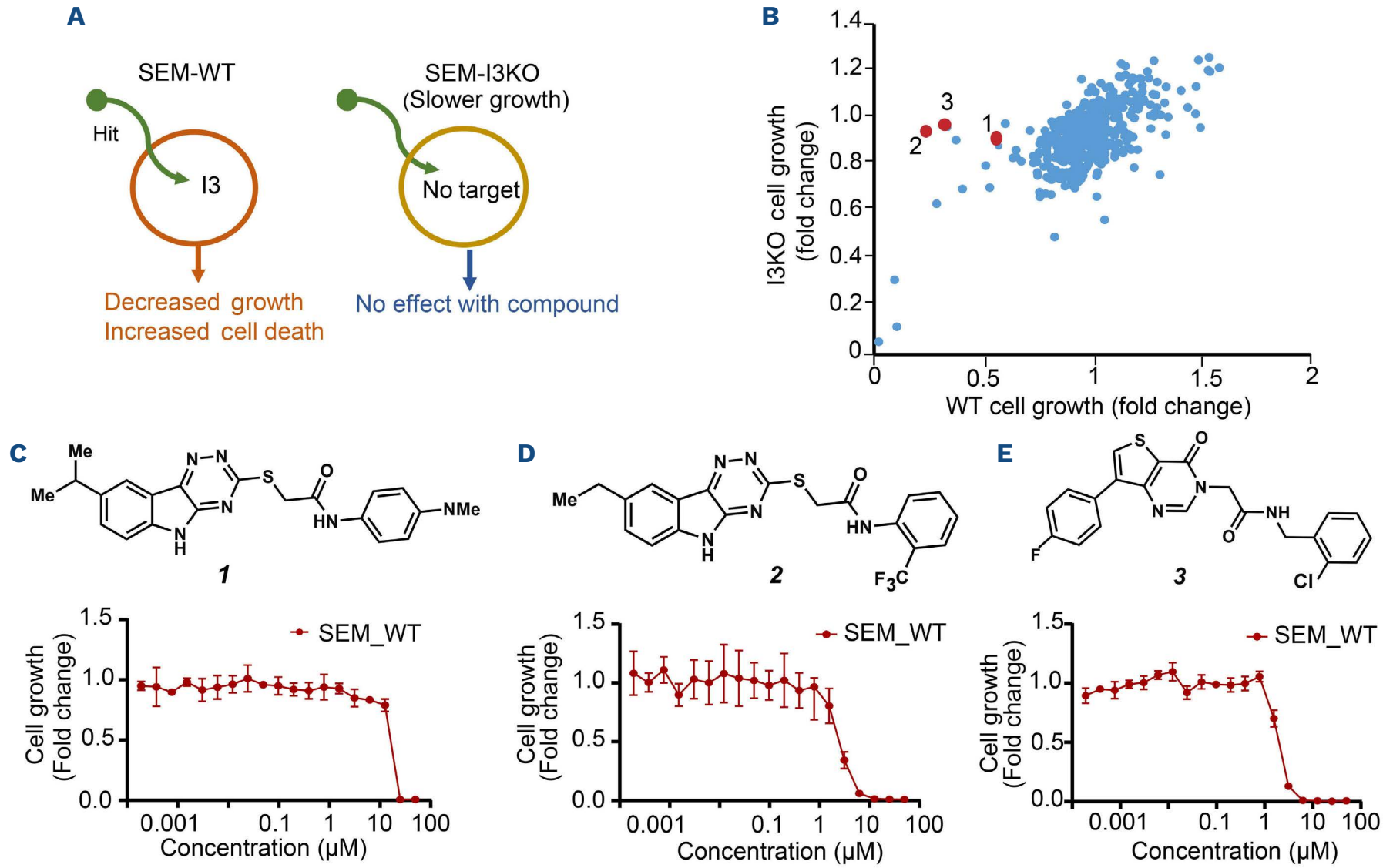

Figure 2. Identification of molecules with biochemical activity and IGF2BP3-dependent anti-proliferative properties. (A) Counter-screen strategy: SEM cells with (SEM-wild-type [WT]) and without IGF2BP3 (SEM-I3 knockout [KO]) are treated in a medium-throughput format with the small molecules identified from the biochemical screen. (B) Scatter plot examining the relationship between relative changes in cell growth, measured by CellTiterGlo and normalized to DMSO control, in SEM-WT (x-axis) and SEM-I3KO (y-axis). Compounds 1, 2 and 3 (red) were noted to have a preferential effect on SEM-WT and a lesser effect in SEM-I3KO. Cells were treated with 5 μM solutions of test compounds. (C-E) Structures of compounds 1, 2 and 3 (top) and corresponding concentration-dependent changes in cell growth rate (bottom) for the three compounds with favorable characteristics on screening. Growth rate was measured using CellTiterGlo and normalized to DMSO control in SEM-WT cell line.

in cell lines with experimental deletion via CRISPR-Cas9 (SEM-I3KO). Cells were treated with compound, grown for four days under normal growth conditions, and assayed for cell growth with CellTiter-Glo, a luminescence-based reagent described previously.[6,13,14] Fold change from control (i.e., no compound-treated wells) was plotted for SEM-WT *versus* SEM-I3KO. Remarkably, there were compounds that showed enhanced reduction of cell growth in SEM-WT, as opposed to SEM-I3KO (Figure 2B). Using the cutoff (Growth Ratio<0.7 or WT Growth<0.7), we identified 16 compounds. We then chose three promising compounds, designated 1, 2 and 3 here, and tested them across a range of concentrations on SEM cells (Figure 2C-E). Of these, 2 and 3, which we later designated as I3IN-002 and I3IN-003, showed differential activity in the two cell lines, with 2 showing a promising IC_{50} of approximately 2 μM in wild-type SEM-cells (Figure 2D). A summary of the compound screening, validation and selection of the hit compounds is shown in *Online Supplementary Figure S2E*.

I3IN-002 inhibits cell proliferation and cell cycle progression, and promotes apoptosis

To enable further biological evaluation, we sought to prepare I3IN-002 in high purity and in larger quantities than those available commercially. Moreover, chemical characterization data for I3IN-002 was not identified in the literature. To access I3IN-002, we performed the synthetic route shown in Figure 3A. First, isatin (Figure 3A, 4) was treated with thiosemicarbazide (Figure 3A, 5) and potassium carbonate in methanol at ambient temperature to give hydrazone formation. The hydrazone intermediate was subjected to potassium carbonate in water at reflux to give triazinoindolothione (Figure 3A, 6).[18] Then, the intermediate compound (Figure 3A, 6) was treated with alkyl chloride (Figure 3A, 7) in the presence of potassium carbonate in DMSO.[19] This delivered I3IN-002, which was isolated as a powder. The purity of I3IN-002 was deemed to be >97% by both quantitative ^{1}H NMR and HPLC analysis.

To characterize the activity of I3IN-002, we tested the

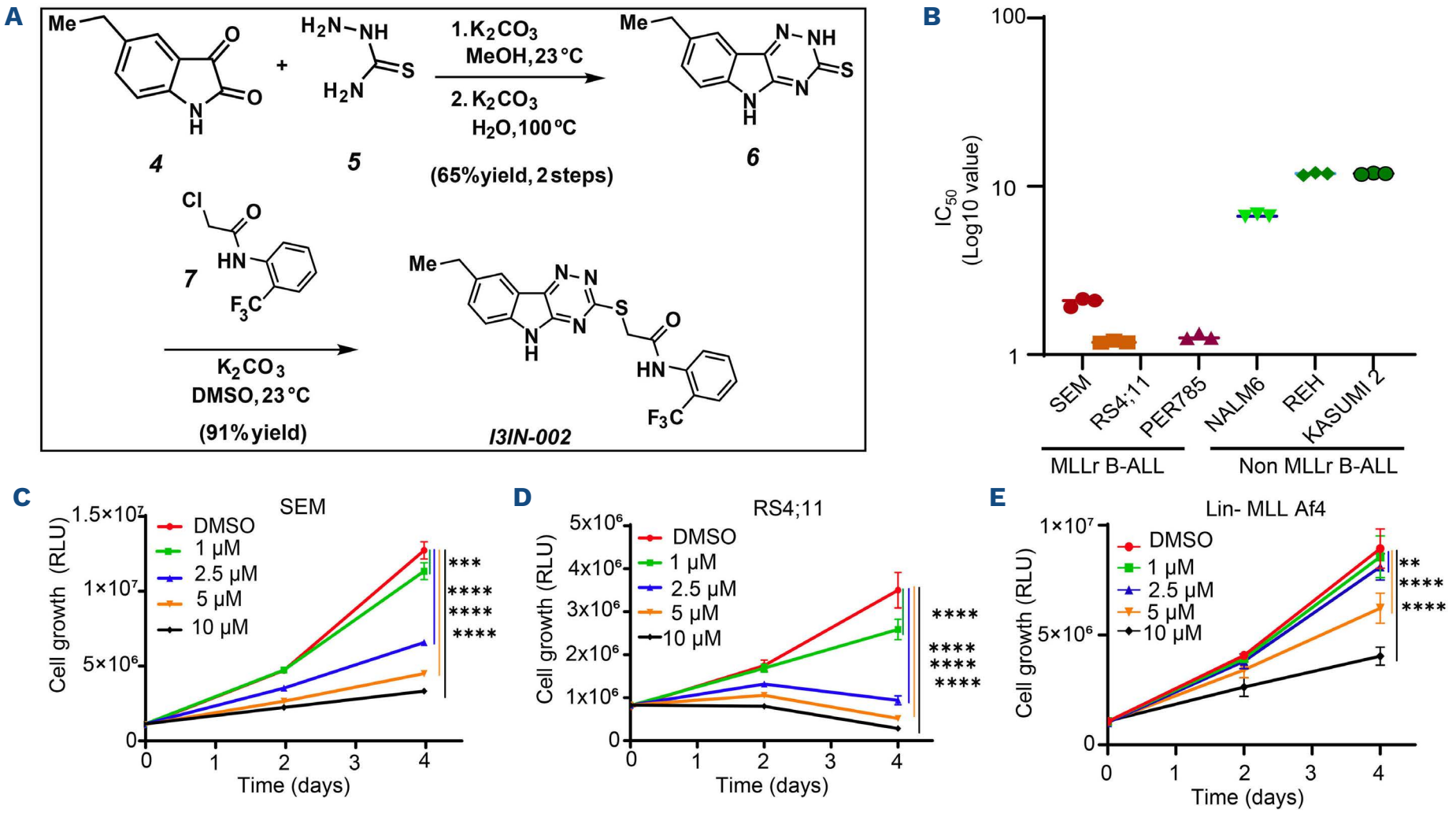

Figure 3. I3IN-002 hampers cell growth in human and mouse leukemic cells. (A) Chemical synthesis of I3IN-002. (B) IC_{50} values of I3IN-002 on MLLr B-cell acute lymphoblastic leukemia (B-ALL) and B-ALL cell lines. (C-E) Concentration-dependent alterations of cell growth curves over four days of cell culture with I3IN-002 treatment, assessed by CellTiterGlo assay, and plotted as relative luminescence units (RLU). SEM (C), RS4;11 (D), and Lin^-/MLL-Af4 (E) cells were assayed in this experiment. Data represent mean and standard error of the mean in 8 replicates. Statistical significance was evaluated by Student *t* test: ***P*<0.01, ****P*<0.001, *****P*<0.0001.

compound in a number of leukemia models, including SEM, RS4;11, PER 785, KASUMI-2, NALM6, REH, and MLL-Af4 Lin^- cells after studying the baseline expression of IGF2BP3 in these cells (*Online Supplementary Figure S3A*). IC_{50} experiments performed on these cell lines showed the compound is more potent in B-cell acute lymphoblastic leukemia (B-ALL) cell lines with MLL-AF4 translocation, with lower IC_{50} values compared to other B-ALL cell lines (Figure 3B). Treatment with a single dose of I3IN-002 resulted in a dose-dependent growth inhibition of SEM, RS4;11 Lin^-MLL-Af4 and MV4;11 cells at the concentrations tested in our assays (Figure 3C-E and *Online Supplementary Figure S3B*). Moreover, cell cycle profiling using propidium iodide in both SEM and RS4;11 cells showed an increase in sub-G0 cells (Figure 4A and *Online Supplementary Figure S3C, D*); changes in other phases of the cell cycle were not as consistent. This may, in part, be because in SEM cells the G2-M transition genes such as CDK1 and CCNB2, which are also regulated by IGF2BP3, were down-regulated due to compound treatment (*Online Supplementary Figure S3E, F*). Next, we analyzed the effect of I3IN-002 on cellular apoptosis. These studies showed an increase in apoptosis, as detected by Caspase 3/7 activity in both SEM and RS4;11 cells (Figure 4B, C). Treatment also led to a numerically small but statistically significant increase in Annexin V^+ cells as well as in necrotic cells (Annexin V^+ and propidium $iodide^+$) in both SEM and RS4;11 cells (Figure 4D and *Online Supplementary Figure S3G, H*). Together, these studies indicate that I3IN-002 impacts cell growth, cell cycle, and apoptosis in a variety of target cell lines, with an enhanced growth inhibitory effect in MLL-AF4-driven leukemia.

Reduction of leukemia-initiating cells and leukemia engraftment *in vivo* by I3IN-002

Given our previous work showing that genetic ablation of *Igf2bp3* led to a reduction in leukemia initiating cells, we next assayed whether I3IN-002 caused an effect on plating efficiency in methylcellulose colony formation assays. Similar to genetic knockout, I3IN-002 treatment led to a reduction in total colony counts in a dose-dependent manner and a reduction in the fraction of cells that showed expression of CD34 and c-kit (Figure 4E, F and *Online Supplementary Figure S3 I*). We also observed a reduction in the $CD34^+CD38^+$ fraction (thought to correspond to leukemic stem cells in OCI-AML8227 cells[20]) (*Online Supplementary Figure S3J, K*).

With these findings, we next evaluated the compound *in vivo*. For *in vivo* experiments, mice syngeneically transplanted with the Lin⁻MLL-Af4 cells (either WT or I3KO) (*Online Supplementary Figure S4A*) were injected intraperitoneally with I3IN-002 or vehicle control using the schedule indicated (Figure 5A). This model demonstrates a rapid and lethal leukemia that primarily involves the bone marrow and spleen, with lesser involvement of the peripheral blood. Here, we used the genetic deletion of *Igf2bp3* as a positive control for the predicted effect of IGF2BP3 inhibition, as genetic ablation prevents leukemia development.[13,14] Upon harvest at four weeks post transplant, WT-transplanted mice that received I3IN-002 showed significantly reduced spleen size and weight compared to vehicle-treated control mice, but larger than I3KO-transplanted mice (Figure 5B, C). FACS analysis revealed that *in vivo* treatment reduced the number of CD34⁺ c-kit⁺ cells in both the spleen and the bone marrow (Figure 5D and *Online Supplementary Figure S4B*).

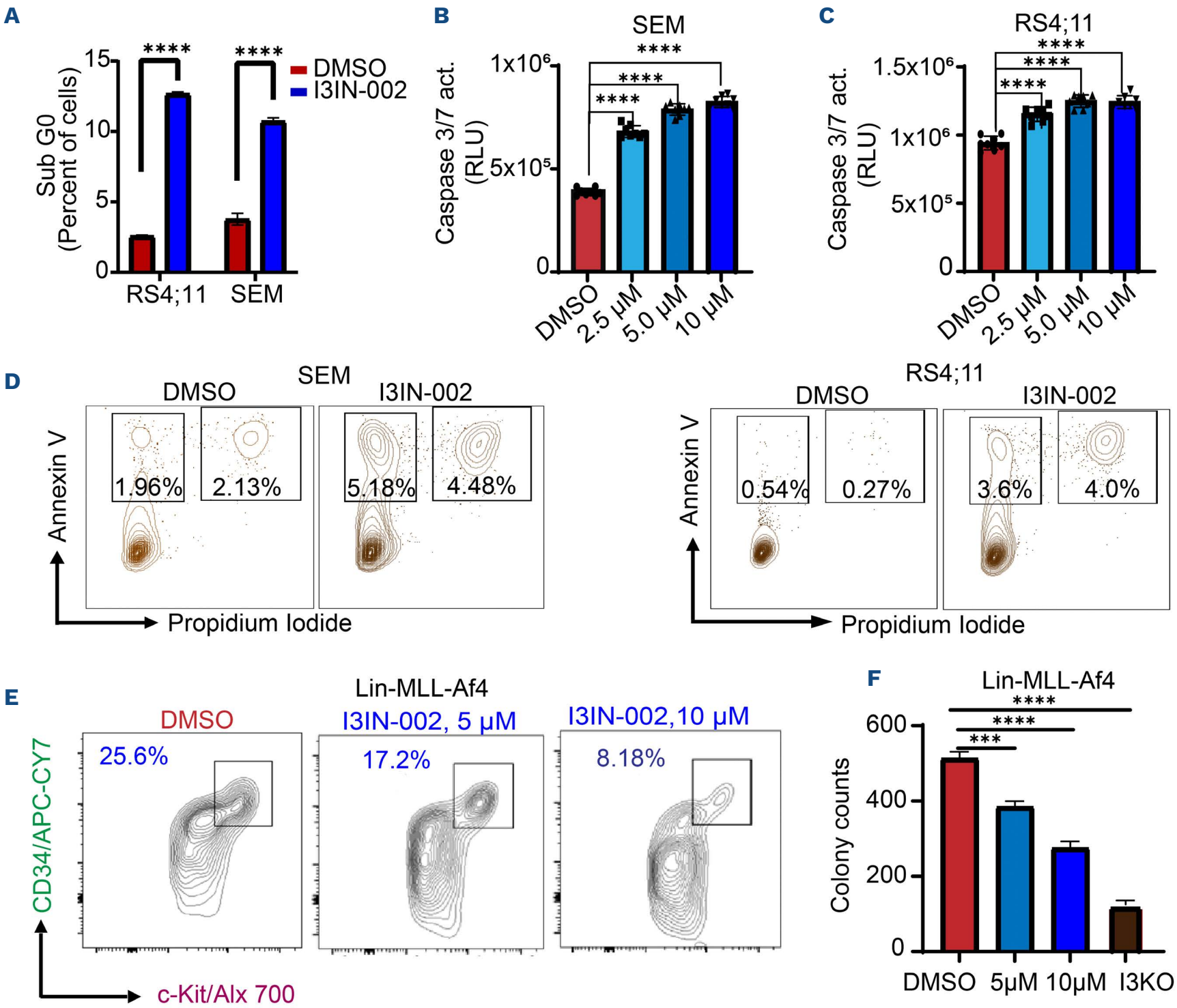

Figure 4. I3IN-002 treatment causes cell cycle arrest and apoptosis in human and mouse leukemic cells. (A) Measurement of sub-G0 cells by propidium iodide staining in SEM and RS4;11 cells, respectively, following treatment with 5 μM I3IN-002 or DMSO. Data represent mean and standard error of the mean of the calculated percentage of cells at each stage of cell cycle with 3 replicates. (B and C) Measurement of apoptosis induction, by Caspase 3/7 activity assay in SEM and RS4;11cells. Data represent mean and standard error of mean with 8 replicates. (D) Measurement of cell death by orthogonal method of Annexin V and propidium iodide staining in SEM and RS4;11 cells. Shown are the % of cells that are single or double positive for propidium iodide and Annexin V. (E) Quantitation of a leukemic stem-cell enriched population by assaying the CD34⁺ c-kit⁺ population following *in vitro* treatment of Lin⁻/MLL-Af4 cells in culture. (F) Measurement of colony formation in methylcellulose following treatment of a murine model of MLL-Af4-driven leukemia[14] with I3IN-002. Data represent the mean number of total colonies for each condition, with 3 replicates per condition. I3KO represents genetic knockout of IGF2BP3, which results in reduced colony formation. Statistical significance was evaluated by Student *t* test: ***P<0.001, ****P<0.0001.

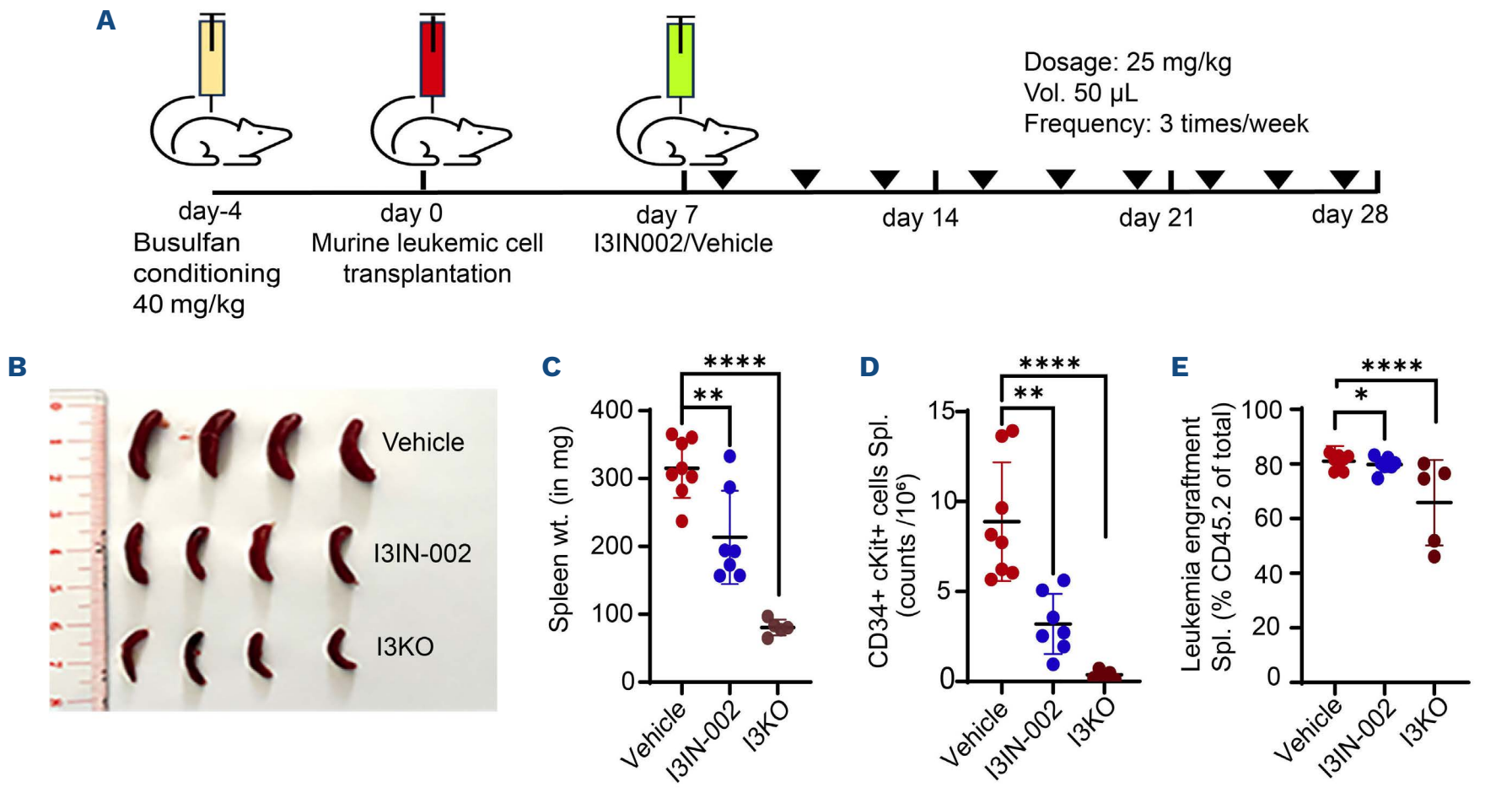

Figure 5. I3IN-002 inhibits leukemic growth *in vivo*. (A) Schematic of mouse experiment. (B) Gross pathology photographs of murine spleens from mice syngeneically transplanted with Lin⁻/MLL-Af4 cells. I3KO are genetic knockouts of IGF2BP3, which markedly reduced leukemic engraftment. (C) Splenic weights from treated mice, as indicated. (D) FACS staining for CD34 and c-kit in the spleen of treated mice, as indicated. (E) Quantification of overall leukemia engraftment in the spleen. (F) Histology of liver (top) and spleen (bottom) from treated mice, as indicated. Arrow indicates a leukemic infiltrate in the liver in the portal area. Dotted lines indicate splenic white pulp, with leukemic infiltrates in the red pulp (area outside the dotted lines). Hematoxylin and eosin staining, original magnification, 200X. (G) Kaplan-Meier survival curve shows effect of I3IN-002 injection on overall survival in syngeneic bone marrow transplant experiment. Data in (C-E) represent one experiment composed of the following numbers of animals: Vehicle, N=8; I3IN-002, N=7; I3KO, N=5. Statistical significance in (C-E) was evaluated by Student *t* test:**P*<0.05; ***P*<0.01; ****P*<0.001; *****P*<0.0001. In (G), Kaplan Meier Survival analysis (N=12 mice/group) was performed with log-rank test. ****P*<0.001.

In the spleen, leukemic engraftment (Figure 5E and *Online Supplementary Figure S4C*) and the proportion of CD11b⁺ cells (*Online Supplementary Figure S4D, E*) and of CD34⁺ Sca1⁻ cells were reduced significantly (*Online Supplementary Figure S4F*). In the bone marrow, there was no difference in overall leukemic engraftment following I3IN-002 treatment compared to vehicle (*Online Supplementary Figure S4G*), but significant reductions in CD11b⁺ and CD34⁺ Sca1⁻ cells were noted (*Online Supplementary Figure S4H, I*) Histologically, we observed lower levels of leukemic engraftment in the liver (*Online Supplementary Figure S4H, I*; compare cellular area next to arrow), and reduced architectural distortion and lower leukemic engraftment in the spleen (*Online Supplementary Figure S4H, I*; compare size of dotted areas and intervening cellularity) in I3IN-002 treated mice, and, as expected, in I3KO (Figure 5F). Similar reductions in engraftment were also noted in lung and kidney (*Online Supplementary Figure S4J*). Notably, we found significant improvement in overall

survival following I3IN-002 treatment in a separate set of endpoint experiments (Figure 5G). Together, these data indicate a significant effect of I3IN-002 on leukemic burden, corresponding with a reduction in the leukemic-initiating cell fraction, thus inhibiting leukemogenesis and extending survival.

I3IN-002 inhibits IGF2BP3-dependent gene expression changes

Prior work by our group and others[14,21] has shown that IGF2BP3 functions in post-transcriptional gene regulation by binding to mRNA molecules and regulating their expression. To understand the downstream consequences of IGF2BP3 inhibition, we performed RNA-seq of DMSO-treated, I3IN-002-treated and I3KO SEM cells (*Online Supplementary Figure S5A*). These studies resulted in the identification of differentially expressed genes between SEM-WT and SEM-I3KO (N=319 genes) as well as between SEM-WT- and SEM-WT-I3IN-002-treated cells (N=226 genes). Volcano plots demonstrate that the overall changes in gene expression were more pronounced in the genetic knockout of IGF2BP3 compared to I3IN-002-treated cells (Figure 6A). Remarkably, 63 genes were common between the two datasets, which represents a highly significant overlap (nearly 28% of genes regulated by I3IN-002-treatment; Hypergeometric test, *P* value $<10^{-1}$) (Figure 6B; see also *Online Supplementary Figure S5B*). Gene set enrichment analyses of the overlap genes between I3KO and I3IN-002-treated cells showed many pathways that we have previously associated with IGF2BP3 function, including response to oxidative stress, cell activation, cellular response to cytokine stimulus, and neutrophil degranulation (Figure 6C). By RT-qPCR, we noted concordant changes in mRNA levels of *P4HA1*, *BTG2*, *KDM3A*, *BNIP3L*, *TGFBR2*, as well as IGF2BP3 targets *BCL2*, *CDK6*, *MYC*, and *HOXA9*[4,6] (Figure 6D-I and *Online Supplementary Figure S5C-E*). Next, to examine these findings at the protein level, we performed western blotting for three of the proteins encoded by the altered mRNA, finding a decrease in the levels of P4HA1, BTG2, and KDM3A with both I3IN-002 treatment and I3KO (Figure 6J). These protein-level changes were also observed for previously identified targets of IGF2BP3, CDK6 and BCL2 (Figure 6K). Paralleling the findings in cell culture, *Cdk6, Myc, Hoxa9, Kdm3a, Bnip3l* and *Bcl2* mRNA, were down-regulated in spleen samples from mice treated with I3IN-002, based on RT-qPCR (*Online Supplementary Figure S5F-K*).

I3IN-002 inhibits the molecular function of IGF2BP3 in gene regulation

To test how I3IN-002 impacts IGF2BP3 function, we also performed RNA immunoprecipitation (RIP) following treatment with I3IN-002 (Figure 7A). Following confirmation of IGF2BP3 pull-down after immunoprecipitation, we subjected the co-immunoprecipitated RNA to high-throughput sequencing (RIP-seq).[17] The analysis allowed us to identify mRNA that were significantly enriched in the immunoprecipitated fraction (*P* adjusted<0.01), for which we calculated enrichment ratios (fold change of immunoprecipitated RNA *vs*. input RNA). Genes found to be enriched in the control sample (DMSO) were designated as I3 RIP targets. Comparison of these targets with previously identified targets of IGF2BP3 determined by enhanced cross-link-immunoprecipitation and RNA sequencing (eCLIP-seq) in these same cells showed a highly statistically significant overlap (489/772 I3eCLIP-seq targets also seen by RIP-seq; Hypergeometric test $P<10^{-16}$) (Figure 7B). With confidence that RIP-seq had identified known I3 targets, we proceeded to compare the enrichment ratios between the two conditions, finding that the overall degree of up- and down-regulated transcripts were roughly the same. However, we noted that the more highly enriched transcripts, as well as those with a higher difference in enrichment ratios between conditions, showed a skewing towards decreased enrichment in the I3IN-002-treated samples. When we limited the analysis to those transcripts with a difference in enrichment ratios >1 and that were also targets identified by eCLIP-seq, we found that these were highly enriched for transcripts whose interactions with I3 were inhibited (Figure 7C). Using individual qPCR, we found that 4 mRNA that we have previously found to be associated with IGF2BP3, *BCL2*, *CDK6*, *MYC*, and *HOXA9*, as well as genes such as *PAICS* and *HMGA1* identified from the RIP-seq, were decreased in the immunoprecipitate following IGF2BP3 pulldown (Figure 7D and *Online Supplementary Figure S6A-D*). Downstream of binding, IGF2BP3 modulates protein expression of its target transcripts, up-regulating the expression of oncogenes such as *BCL2*, *CDK6*, *HOXA9*.[4,14] Using a 3'UTR-luciferase reporter assay, we found that I3IN-002 inhibits protein expression linked to target 3'UTR of *CDK6*, *BNIP3L*, and *BCL2*, suggesting a concordant functional effect of compound treatment (Figure 7E). Next, to assess *in situ* binding of I3IN-002 to IGF2BP3, we performed a cellular thermal shift assay, finding a difference in thermal stability, as assessed by western blot and quantitation (Figure 7F and *Online Supplementary Figure S6E*). Direct interaction of I3IN-002 with IGF2BP3 was confirmed using orthogonal methods. Thermal shift assay (TSA) using purified full length IGF2BP3 demonstrated stabilization of IGF2BP3 with compound (Figure 7G and *Online Supplementary Figure S6F*), while DARTS demonstrated I3IN-002-dependent inhibition of protease-mediated degradation of IGF2BP3 (*Online Supplementary Figure S6G*). Together, these findings support a mechanism wherein I3IN-002 is impacting the function of IGF2BP3 in its critical role as a post-transcriptional regulator of mRNA homeostasis.

Discussion

The RNA binding protein IGF2BP3 is a potent oncofetal protein, as demonstrated by our work and that of many

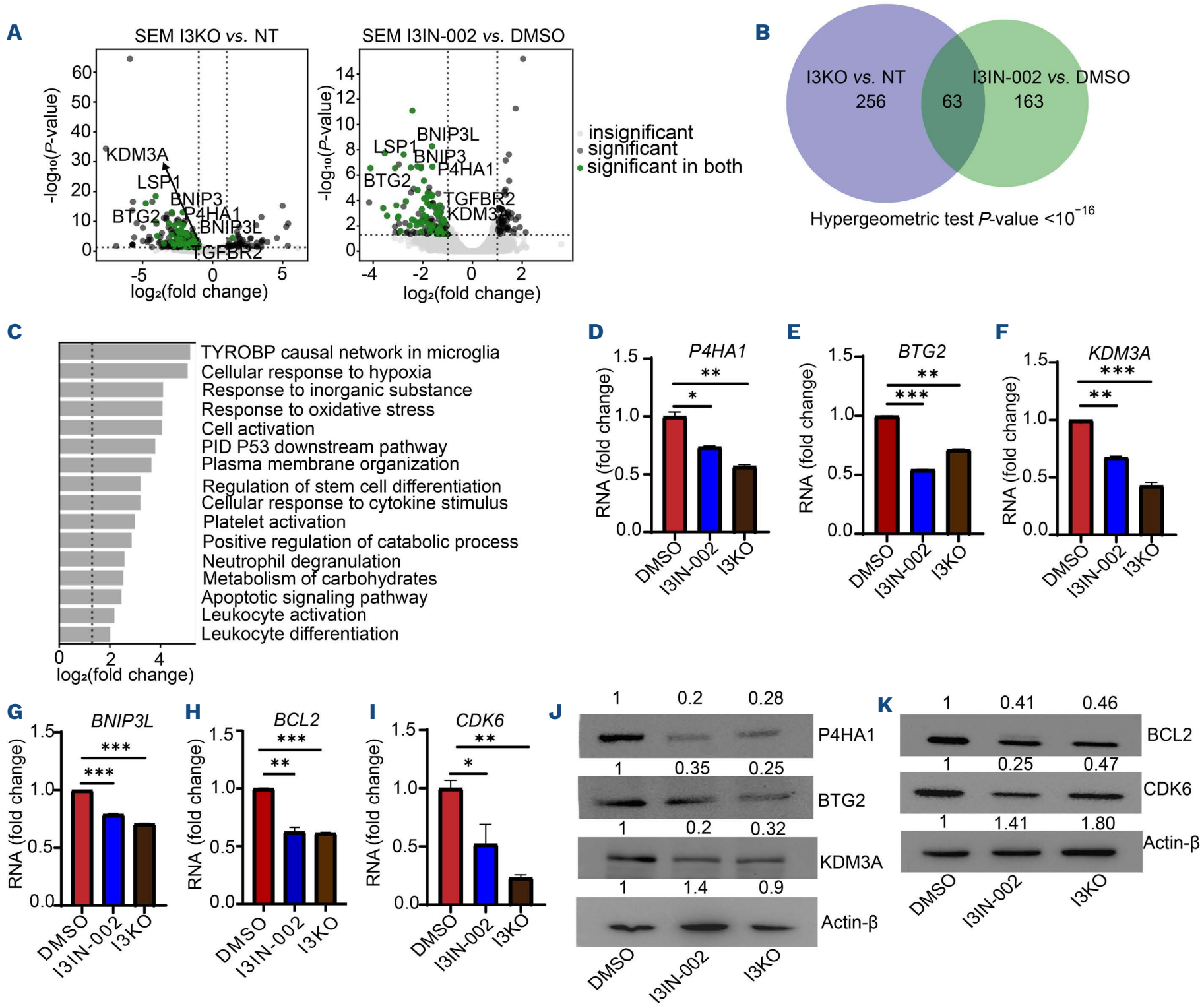

Figure 6. I3IN-002 alters gene expression similar to the genetic knockout. (A) Volcano plots of differentially expressed genes with genetic IGF2BP3 knockout (KO) (left) and with I3IN-002 treatment (right) in SEM cells, using DESeq analysis on RNA-sequencing data from SEM cells treated with DMSO, I3IN-002 and SEM/I3KO. (B) Venn diagram of shared differentially expressed genes with IGF2BP3 knockout and I3IN-002 treatment in SEM cells. Hypergeometric test of overlap showed a *P* value<10^{-16}. (C) Gene Set Enrichment Analysis analysis of the overlapped genes between I3KO and I3IN-002 treated cells. (D-I) Reverse transcription-quantitative polymerase chain reaction-based confirmation of genes showing common differential regulation between I3IN-002 treatment and genetic knockout of IGF2BP3 (I3KO). Data are shown as fold change, following normalization to DMSO, with 3 replicate measurements per sample. (J and K) Western blot measurement of differential genes from RNA-seq experiment P4HA1, BTG2, KDM3A, and known IGF2BP3 targets BCL2 and CDK6. Statistical significance was evaluated by Student *t* test:**P*<0.05; ***P*<0.01; ****P*<0.001.

others.[3,4,6,21] In this manuscript, we describe the successful completion of a high-throughput biochemical screening assay that utilizes the RNA binding function of IGF2BP3 as the discriminant for small molecule activity. Combining the biochemical screen with a cell-based assay to detect IGF2BP3-dependent effects on leukemic cell growth and survival, we identified 16 compounds that are likely to have activity in an IGF2BP3-specific manner. The first of these compounds to be confirmed is I3IN-002, which shows an IC_{50} of approximately 2 μM in initial assays. Specifically, I3IN-002 inhibited cell growth, impacted cell cycle progression of treated cells, and increased apoptosis. I3IN-002 inhibited leukemia-initiating cells and showed *in vivo* anti-leukemic activity. Furthermore, I3IN-002 impacted global gene expression in a manner similar to genetic deletion of IGF2BP3. CETSA, TSA, DARTS, and RNA immunoprecipitation experiments supported on-target activity against IGF2BP3. RNA-binding proteins have recently been recognized as

biologically and clinically significant regulators of gene expression.[12,21-23] This has led to a growing effort to target RNA-binding proteins, but challenges remain.[12,24] First, many cancer-associated RNA-binding proteins are also required for normal homeostasis[25] and hence, targeting these proteins might engender significant toxicity. The IGF2BP family of proteins has emerged as cancer-specific or cancer-enriched proteins, and IGF2BP3 is an oncofetal protein, making this an attractive cancer target. Second, while oligonucleotide-based therapies hold great prom-

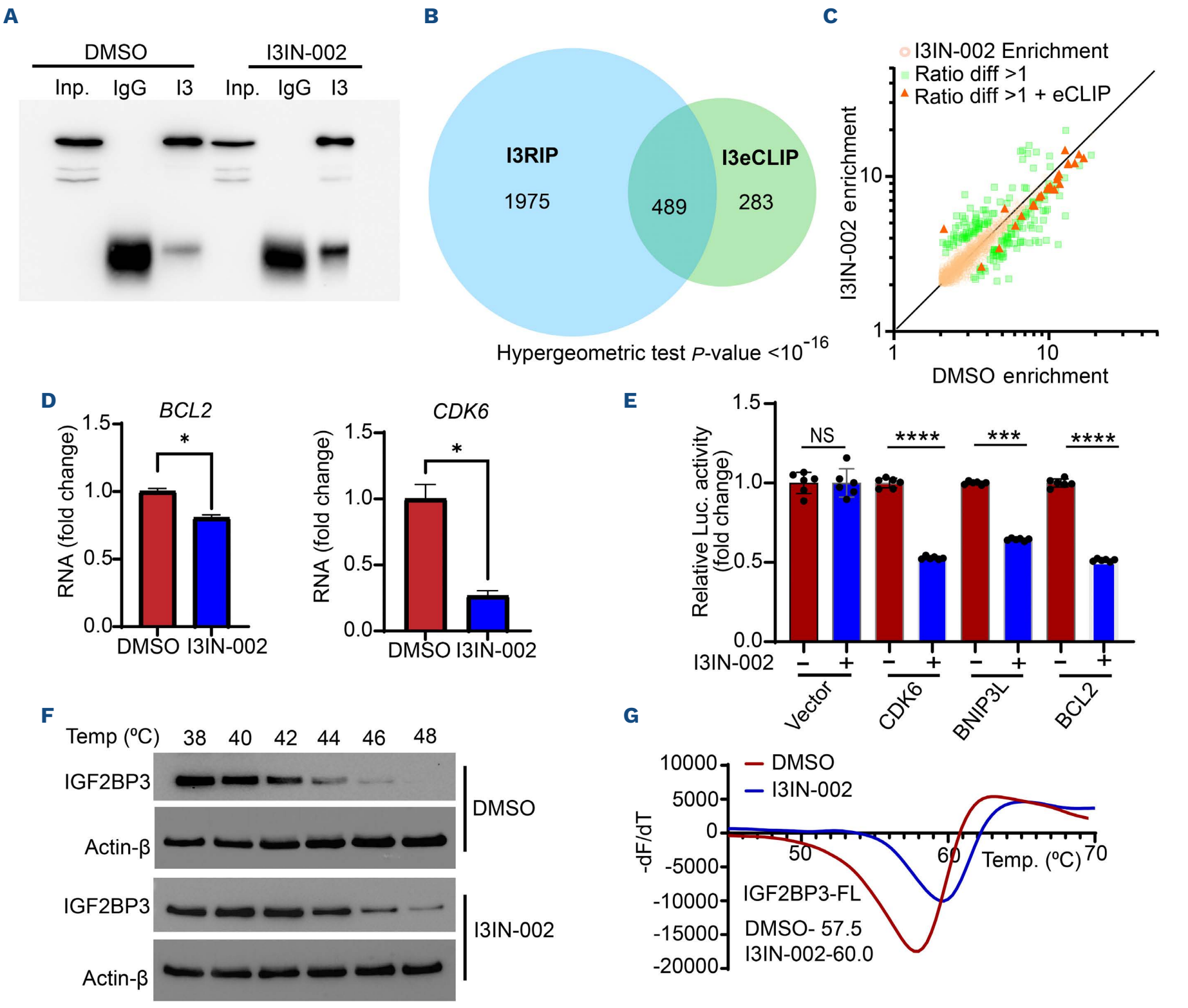

Figure 7. I3IN-002 shows on target activity in biochemical assays. (A) Western blot analysis of RNA immunoprecipitation samples following treatment of SEM cells with 5 μM I3IN-002. Inp: input cell lysate; IgG; a control immunoprecipitation with isotype control; IP:anti-IGF2BP3 immunoprecipitation. (B) Venn diagram showing significant overlap of differentially expressed genes from I3RIP and I3eCLIP. Hypergeometric test of overlap showed a *P* value $<10^{-16}$. (C) Scatter plot of RIP-seq data, plotted as enrichment ratio in DMSO-treated cells (x-axis) *versus* enrichment ratio in I3IN-002-treated cells (orange dots). Differentially enriched genes with a difference in enrichment ratio of >1 between I3IN-002 and DMSO are shown as green squares. Red triangles indicate genes with an enrichment ratio difference of >1 as well as being identified as IGF2BP3 target mRNA on prior eCLIP analysis. (D) Quantification of *CDK6* and *BCL2* RNA recovered from RNA immunoprecipitation experiments with or without treatment with I3IN-002. (E) Dual luciferase assay on 3' UTR of IGF2BP3 targets show decrease in Relative Luciferase activity in the presence of I3IN-002, calculated as Firefly luciferase / Renilla luciferase ratio, and expressed as fold change from DMSO for each UTR. NS: not significant; Vector: empty vector with no 3'UTR, used here as a negative control. Data represent mean and standard error of mean from 6 replicates. (F) Cellular thermal shift assay; western blots of IGF2BP3 and β-actin are shown following treatment of cells with I3IN-002 or DMSO control, followed by heat-mediated denaturation and removal of denatured protein. (G) Thermal shift assay using purified full-length IGF2BP3 protein. Statistical significance was evaluated by Student *t* test:*P<0.05; ***P<0.001; ****P<0.0001.

ise, targeting of many tissues, including cancer, remains a major challenge in the field. Hence, small molecule therapeutics holds many advantages, including delivery and bioavailability, with the development of reproducible and straightforward synthesis methods allowing for future large-scale manufacturing and distribution. Our efforts here have resulted in some of the first small molecules identified by empirical, experimental approaches to target IGF2BP3. Moreover, the molecule identified here, I3IN-002, is effective at inhibiting the protein-RNA interaction, as measured by multiple reporter assays. We suggest that this parameter may be a critical and useful measure of efficacy of small molecules for targeting post-transcriptional regulation.

In recent years, several small molecules have been reported to inhibit the IGF2BP family of proteins. Regulators of expression include an isocorydine derivative, 8-amino-ICD, which was reported to target hepatocellular carcinoma and decrease IGF2BP3 expression at an EC_{50} of 20 μM or greater.[26] In non-small cell lung cancer, isoliquiritigenin is also able to down-regulate IGF2BP3 expression in a dose-dependent manner.[27] Most recently, a virtual screening approach identified AE-848 as an inhibitor of IGF2BP3 with an IC_{50} of approximately 10-40 μM in ovarian cancer.[28] Other IGF2BP proteins have been reported to be targeted by small molecules: BTYNB targets IGF2BP1 (IC_{50} of 5-10 μM); JX1 targets IGF2BP2 (IC_{50} of 10-20 μM) in acute T-lymphoblastic leukemia, and CWI1-2 also targets IGF2BP2 (sub-micromolar IC_{50} in acute myeloid leukemia [AML] cell lines).[29-31] Our discoveries here indicate that I3IN-002 is the most potent inhibitor of IGF2BP3 reported to date, and the first in hematologic malignancy, and strongly support its role in altering oncogenic post-transcriptional gene regulation, providing the impetus for further drug discovery efforts.

Biologically-active small molecules containing indolyltriazine cores possess potent and selective activity across a variety of indications. Other anti-cancer compounds containing the motif include an inhibitor of tyrosine phosphatase SHP-2,[32] and a commercially available tool compound, Inauhzin, which acts as a SIRT-1 inhibitor.[33] Furthermore, this motif has also been found in antibiotics, α-glucosidase inhibitors, and targeted P-glycoprotein inhibitors, amongst other classes of biologically relevant molecules.[18,34-36] Notably, many of these compounds are demonstrated to be highly selective. This relatively diverse set of targets is consistent with our findings that small changes in the structure can markedly alter the bioactivity of the indolyltriazine in acute leukemia (i.e., only 2 out of 29 TR-FRET-active indolyltriazine compounds tested showed bioactivity). In other words, the specificity of the compounds may be highly malleable with chemical modifications of the side chains. Our initial efforts indicate that I3IN-002 can be readily synthesized using widely available commercial component molecules. This information should enable future efforts to develop compound analogs of I3IN-002 that display selective binding to IGF2BP3, without off-target effects. Importantly, while the indolyltriazine core is seemingly privileged with respect to bioactivity, it is not found in any commercially available drugs to date.

It is also of interest to note that we recently showed that IGF2BP3 genetic ablation was additive with menin inhibition in MLL-AF4 leukemia.[14] While outside the scope of this report, compounds generated here could, therefore, be useful in combinatorial therapeutic approaches with menin inhibition, inhibiting leukemia at the transcriptional and post-transcriptional levels. In addition, IGF2BP3 targets include a number of key oncogenic proteins, which are themselves the targets of advanced small molecule development programs. For example, CDK6 is a direct target of IGF2BP3 that is up-regulated by the latter's activity, and anti-CDK4/6 inhibitors have been developed as potent agents in cancer therapy, for example, in breast cancer.[37] BCL2 is also a direct target of IGF2BP3, and the BCL2 inhibitor venetoclax has shown activity in a number of hematologic malignancies, including B-ALL and AML. Other IGF2BP3 targets, such as MYC, which have long been elusive as drug targets, are also now being actively pursued with small molecule approaches.[38] Hence, our development of IGF2BP3 small molecule inhibitors could be especially important in future combinatorial therapy approaches, which is an important future direction for our work.

While this work contains important advances, showing that disrupting IGF2BP3-RNA binding can be the basis of a therapeutic approach in selected hematologic malignancies, we acknowledge that there are areas for important future work. *In vitro* studies of binding affinities have yet to be completed, due to difficulties in purifying full-length protein in quantities sufficient for detailed biochemical analyses. We believe this is because the protein may be prone to liquid-liquid phase separation, and prior work has focused on individual domains within the protein, yielding crystal structures of protein subdomains only.[39-42] Moreover, pharmacological parameters of this compound and its derivatives will require optimization. Thus, future directions will involve analog synthesis and biochemical evaluation to ultimately improve and validate selective binding to IGF2BP3, while also optimizing drug-like properties.

Overall, our study has led to the discovery and validation of I3IN-002, a small molecule that inhibits IGF2BP3-RNA interactions. While our work has thus far focused on the role of IGF2BP3 in acute leukemia, it is known that IGF2BP3 is over-expressed in a range of B-cell malignancies, including diffuse large B-cell lymphoma, Burkitt lymphoma, and others.[43-45] Moreover, it is estimated that up to 15% of all human cancers over-express IGF2BP3, including both hematologic and non-hematologic malignancies, with high levels correlated with aggressive tumor behavior by expression and functional analyses.[3,21,46-50] Consistent with the notion of being an oncofetal protein, our work has determined that IGF2BP3 appears to be largely dispensable in homeostatic development,[6] providing a significant

therapeutic window for targeting. It should be noted that IGF2BP3 expression is quite variable within different types of cancer, and hence, future indications will need to be carefully defined. We speculate that IGF2BP3 expression could be evaluated in different cancer types by widely available techniques such as immunohistochemistry, and compounds such as I3IN-002 or future derivatives could be administered as a precision medicine intervention in carefully selected patients. Hence, I3IN-002 serves as a promising lead compound for future drug discovery efforts aimed at identifying selective inhibitors of IGF2BP3, particularly for the treatment of acute leukemia.

Disclosures

DSR serves on advisory boards and has had a consultancy role for AbbVie Inc., a pharmaceutical company that markets drugs for acute leukemia. AKJ, MLT, GMS, JPS, RDD, NKG and DSR are inventors on a patent application that includes the compound I3IN-002. All of the other authors have no conflicts of interest to disclose.

Contributions

AKJ designed research, performed experiments, acquired and analyzed data, generated the figures, led the experiments, and wrote the manuscript. GMS performed experiments, acquired and analyzed data, and assisted in generating figures. MLT, JPS and MMM performed experiments, and acquired and analyzed data. CY, GS and TMT performed experiments. TLL and AC performed experiments and acquired data. AJR and JRS analyzed data. RSK provided the MLL AF4 B-ALL cell line. RDD designed research and analyzed data. NKG designed research, analyzed data, and edited the manuscript. DSR designed research, analyzed data, wrote the manuscript, secured funding, and led the project.

Acknowledgments

We thank Dr. Stuart Conway and Keefe Oei for helpful conversations, advice and protocols for biophysical assays. We thank Jaspal Bassi and Dr. John Colicelli for helpful discussions regarding the research.

Funding

This work was supported by CIRM DISC-2-13456 from the California Institute of Regenerative Medicine (to DSR), R01CA264986 from the National Institutes of Health (to DSR and JRS), R03CA251854 (to DSR), the Jonsson Comprehensive Cancer Center (JCCC) (to DSR), the Gary & Barbara Luboff Mitzvah Fund (to DSR) and the UCLA Innovation Fund Award (to DSR). Flow cytometry was performed in the UCLA JCCC and Center for AIDS Research Flow Cytometry Core Facility that is supported by National Institutes of Health awards AI28697, and award number P30CA016042, the JCCC, the UCLA AIDS Institute, and the David Geffen School of Medicine at UCLA. We are especially indebted to the Molecular Screening Shared Resource team for setup and execution of small molecule-related screening assays. The MSSR is also supported by the Jonsson Comprehensive Cancer Center (NIH award number P30CA016042, Cancer Center Support Grant). These studies were also supported by the National Science Foundation (DGE-2034835 for GMS and DGE-1650604 for MMM), shared instrumentation grants from the NSF (CHE-1048804), the National Center for Research Resources (S10RR025631), and the NIH Office of Research Infrastructure Programs (S10OD028644).

Data-sharing statement

High throughput sequencing data has been deposited in the NCBI Short Read Archive (BioProject PRJNA1333638 and PRJNA1336320) and will be released upon publication. Methodologies are documented in the Online Supplementary Appendix and further information can be provided by the corresponding author. Biological or chemical materials that were created in the process of this work can be requested from the corresponding author and will be released following compliance with relevant intellectual property and material transfer policies.

References

1. Müeller-Pillasch F, Lacher U, Wallrapp C, et al. Cloning of a gene highly overexpressed in cancer coding for a novel KH-domain containing protein. Oncogene. 1997;14(22):2729-2733.
2. Nielsen J, Christiansen J, Lykke-Andersen J, Johnsen AH, Wewer UM, Nielsen FC. A family of insulin-like growth factor II mRNA-binding proteins represses translation in late development. Mol Cell Biol. 1999;19(2):1262-1270.
3. Mancarella C, Scotlandi K. IGF2BP3 from physiology to cancer: novel discoveries, unsolved issues, and future perspectives. Front Cell Dev Biol. 2020;7:363.
4. Palanichamy JK, Tran TM, Howard JM, et al. RNA-binding protein IGF2BP3 targeting of oncogenic transcripts promotes hematopoietic progenitor proliferation. J Clin Invest. 2016;126(4):1495-1511.
5. Stoskus M, Gineikiene E, Valceckiene V, Valatkaite B, Pileckyte R, Griskevicius L. Identification of characteristic IGF2BP expression patterns in distinct B-ALL entities. Blood Cells Mol Dis. 2011;46(4):321-326.
6. Tran TM, Philipp J, Bassi JS, et al. The RNA-binding protein IGF2BP3 is critical for MLL-AF4-mediated leukemogenesis. Leukemia. 2022;36(1):68-79.
7. Lin S, Luo RT, Ptasinska A, et al. Instructive role of MLL-fusion proteins revealed by a model of t(4;11) pro-B acute lymphoblastic leukemia. Cancer Cell. 2016;30(5):737-749.
8. Yang Z, Wang T, Wu D, Min Z, Tan J, Yu B. RNA N6-methyladenosine reader IGF2BP3 regulates cell cycle and angiogenesis in colon cancer. J Exp Clin Cancer Res. 2020;39(1):203.
9. Huang H, Weng H, Sun W, et al. Recognition of RNA N(6)-methyladenosine by IGF2BP proteins enhances mRNA stability

and translation. Nat Cell Biol. 2018;20(3):285-295.
10. Ren F, Lin Q, Gong G, et al. Igf2bp3 maintains maternal RNA stability and ensures early embryo development in zebrafish. Commun Biol. 2020;3(1):94.
11. Gu Y, Niu S, Wang Y, et al. DMDRMR-mediated regulation of m(6)A-modified CDK4 by m(6)A reader IGF2BP3 drives ccRCC progression. Cancer Res. 2021;81(4):923-934.
12. Elcheva IA, Spiegelman VS. Targeting RNA-binding proteins in acute and chronic leukemia. Leukemia. 2021;35(2):360-376.
13. Jaiswal AK, Truong H, Tran TM, et al. Focused CRISPR-Cas9 genetic screening reveals USO1 as a vulnerability in B-cell acute lymphoblastic leukemia. Sci Rep. 2021;11(1):13158.
14. Lin TL, Jaiswal AK, Ritter AJ, et al. Targeting IGF2BP3 enhances antileukemic effects of menin-MLL inhibition in MLL-AF4 leukemia. Blood Adv. 2024;8(2):261-275.
15. Jafari R, Almqvist H, Axelsson H, et al. The cellular thermal shift assay for evaluating drug target interactions in cells. Nat Protoc. 2014;9(9):2100-2122.
16. Pai MY, Lomenick B, Hwang H, et al. Drug affinity responsive target stability (DARTS) for small-molecule target identification. Methods Mol Biol. 2015;1263:287-298.
17. Sharma G, Tran TM, Bansal I, et al. RNA binding protein IGF2BP1 synergizes with ETV6-RUNX1 to drive oncogenic signaling in B-cell acute lymphoblastic leukemia. J Exp Clin Cancer Res. 2023;42(1):231.
18. Rahim F, Ullah K, Ullah H, et al. Triazinoindole analogs as potent inhibitors of alpha-glucosidase: synthesis, biological evaluation and molecular docking studies. Bioorg Chem. 2015;58:81-87.
19. Shelke SM, Bhosale SH. Synthesis, antidepressant evaluation and QSAR studies of novel 2-(5H-[1,2,4]triazino[5,6-b]indol-3-ylthio)-N-(substituted phenyl)acetamides. Bioorg Med Chem Lett. 2010;20(15):4661-4664.
20. Subedi A, Liu Q, Ayyathan DM, et al. Nicotinamide phosphoribosyltransferase inhibitors selectively induce apoptosis of AML stem cells by disrupting lipid homeostasis. Cell Stem Cell. 2021;28(10):1851-1867.e8.
21. Bell JL, Wachter K, Muhleck B, et al. Insulin-like growth factor 2 mRNA-binding proteins (IGF2BPs): post-transcriptional drivers of cancer progression? Cell Mol Life Sci. 2013;70(15):2657-2675.
22. Wang E, Lu SX, Pastore A, et al. Targeting an RNA-binding protein network in acute myeloid leukemia. Cancer Cell. 2019;35(3):369-384.e7.
23. Gebauer F, Schwarzl T, Valcarcel J, Hentze MW. RNA-binding proteins in human genetic disease. Nat Rev Genet. 2021;22(3):185-198.
24. Tran TM, Rao DS. RNA binding proteins in MLL-rearranged leukemia. Exp Hematol Oncol. 2022;11(1):80.
25. Jaiswal AK, Thaxton ML, Scherer GM, Sorrentino JP, Garg NK, Rao DS. Small molecule inhibition of RNA binding proteins in haematologic cancer. RNA Biol. 2024;21(1):1-14.
26. Li M, Zhang L, Ge C, et al. An isocorydine derivative (d-ICD) inhibits drug resistance by downregulating IGF2BP3 expression in hepatocellular carcinoma. Oncotarget. 2015;6(28):25149-25160.
27. Cui Y, Wu Y, Wang C, et al. Isoliquiritigenin inhibits non-small cell lung cancer progression via m(6)A/IGF2BP3-dependent TWIST1 mRNA stabilization. Phytomedicine. 2022;104:154299.
28. Shu C, Gu MH, Zeng C, et al. Small-molecule exhibits anti-tumor activity by targeting the RNA m(6)A reader IGF2BP3 in ovarian cancer. Am J Cancer Res. 2023;13(10):4888-4902.
29. Weng H, Huang F, Yu Z, et al. The m(6)A reader IGF2BP2 regulates glutamine metabolism and represents a therapeutic target in acute myeloid leukemia. Cancer Cell. 2022;40(12):1566-1582.e10.
30. Mahapatra L, Andruska N, Mao C, Le J, Shapiro DJ. A novel IMP1 inhibitor, BTYNB, targets c-Myc and inhibits melanoma and ovarian cancer cell proliferation. Transl Oncol. 2017;10(5):818-827.
31. Feng P, Chen D, Wang X, et al. Inhibition of the m(6)A reader IGF2BP2 as a strategy against T-cell acute lymphoblastic leukemia. Leukemia. 2022;36(9):2180-2188.
32. Yu WM, Guvench O, Mackerell AD, Qu CK. Identification of small molecular weight inhibitors of Src homology 2 domain-containing tyrosine phosphatase 2 (SHP-2) via in silico database screening combined with experimental assay. J Med Chem. 2008;51(23):7396-7404.
33. Zhang Q, Zeng SX, Zhang Y, et al. A small molecule Inauhzin inhibits SIRT1 activity and suppresses tumour growth through activation of p53. EMBO Mol Med. 2012;4(4):298-312.
34. Garzan A, Willby MJ, Ngo HX, et al. Combating enhanced intracellular survival (Eis)-mediated kanamycin resistance of Mycobacterium tuberculosis by novel pyrrolo[1,5-a]pyrazine-based Eis inhibitors. ACS Infect Dis. 2017;3(4):302-309.
35. Li H, Liu J, Liu CF, et al. Design, synthesis, and biological evaluation of membrane-active bakuchiol derivatives as effective broad-spectrum antibacterial agents. J Med Chem. 2021;64(9):5603-5619.
36. Wise JG, Nanayakkara AK, Aljowni M, et al. Optimizing targeted inhibitors of P-glycoprotein using computational and structure-guided approaches. J Med Chem. 2019;62(23):10645-10663.
37. Wang X, Zhao S, Xin Q, Zhang Y, Wang K, Li M. Recent progress of CDK4/6 inhibitors' current practice in breast cancer. Cancer Gene Ther. 2024;31(9):1283-1291.
38. Boike L, Cioffi AG, Majewski FC, et al. Discovery of a functional covalent ligand targeting an intrinsically disordered cysteine within MYC. Cell Chem Biol. 2021;28(1):4-13.e7.
39. Schneider T, Hung LH, Aziz M, et al. Combinatorial recognition of clustered RNA elements by the multidomain RNA-binding protein IMP3. Nat Commun. 2019;10(1):2266.
40. Li X, Guo W, Wen Y, et al. Structural basis for the RNA binding properties of mouse IGF2BP3. Structure. 2025;33(4):771-785.e3.
41. Jia M, Gut H, Chao JA. Structural basis of IMP3 RRM12 recognition of RNA. RNA. 2018;24(12):1659-1666.
42. Zeng WJ, Lu C, Shi Y, et al. Initiation of stress granule assembly by rapid clustering of IGF2BP proteins upon osmotic shock. Biochim Biophys Acta Mol Cell Res. 2020;1867(10):118795.
43. King RL, Pasha T, Roullet MR, Zhang PJ, Bagg A. IMP-3 is differentially expressed in normal and neoplastic lymphoid tissue. Hum Pathol. 2009;40(12):1699-1705.
44. Kosari F, Bakhshi T, Ameli F, Mokhtari M. The utility of IMP3 immunohistochemical staining in differentiating nodular lymphocyte predominant Hodgkin lymphoma from T-cell/histiocyte-rich large B-cell lymphoma. BMC Cancer. 2022;22(1):1359.
45. Saka M, Fujimoto M, Mizoguchi K, et al. Insulin-like growth factor II mRNA-binding protein 3 is a highly sensitive marker for intravascular large B-cell lymphoma: immunohistochemical analysis of 152 pathology specimens from 88 patients. Am J Surg Pathol. 2024;48(6):671-680.
46. Lederer M, Bley N, Schleifer C, Huttelmaier S. The role of the oncofetal IGF2 mRNA-binding protein 3 (IGF2BP3) in cancer. Semin Cancer Biol. 2014;29:3-12.
47. Schaeffer DF, Owen DR, Lim HJ, et al. Insulin-like growth factor 2 mRNA binding protein 3 (IGF2BP3) overexpression in

pancreatic ductal adenocarcinoma correlates with poor survival. BMC Cancer. 2010;10:59.
48. Kobel M, Xu H, Bourne PA, et al. IGF2BP3 (IMP3) expression is a marker of unfavorable prognosis in ovarian carcinoma of clear cell subtype. Mod Pathol. 2009;22(3):469-475.
49. Lochhead P, Imamura Y, Morikawa T, et al. Insulin-like growth factor 2 messenger RNA binding protein 3 (IGF2BP3) is a marker of unfavourable prognosis in colorectal cancer. Eur J Cancer. 2012;48(18):3405-3413.
50. Jonson L, Christiansen J, Hansen TVO, Vikesa J, Yamamoto Y, Nielsen FC. IMP3 RNP safe houses prevent miRNA-directed HMGA2 mRNA decay in cancer and development. Cell Rep. 2014;7(2):539-551.